Electronic Supplementary Information

Oxatub[5,6]arene: Synthesis, Conformational Analysis, and Recognition of C60 and C70

Fei Jia, Dong-Hao Li, Ti-Long Yang, Liu-Pan Yang, Li Dang, and Wei Jiang*
Department of Chemistry, South University of Science and Technology of China (SUSTC), Xueyuan Blvd 1088, Nanshan District, Shenzhen, 518055, P. R. China
**E-mail: jiangw@sustc.edu.cn;*

Table of Contents

1. Experimental Section

1.1 General method

All the reagents involved in this research were commercially available and used without further purification unless otherwise noted. Solvents were either employed as purchased or dried prior to use by standard laboratory procedures. Thin-layer chromatography (TLC) was carried out on 0.25 mm Yantai silica gel plates (60F-254). Column chromatography was performed on silica gel 60 (Tsingdao 40 – 63 nm, 230 – 400 mesh). ^{1}H and ^{13}C NMR spectra were recorded on Bruker Avance-400, 500 spectrometers. All chemical shifts are reported in ppm with residual solvents or TMS (tetramethylsilane) as the internal standards. The following abbreviations were used for signal multiplicities: s, singlet; d, doublet; t triplet; m, multiplet. Electrospray-ionization time-of-flight high-resolution mass spectrometry (ESI-TOF-HRMS) experiments were conducted on an applied biosystems Elite ESI-QqTOF mass spectrometry system. Theoretical calculations were performed by using Gaussion 09[1] with the BMK/6-31G level of theory to optimize the geometry and relative energies. The synthesis and characterization of compound **1**, compound **2**, and **TA4** have been reported.[2]

1.2 Synthesis and Purification of TA5 and TA6

1 M. J. Frisch, G. W. Trucks, H. B. Schlegel, G. E. Scuseria, M. A. Robb, J. R. Cheeseman, G. Scalmani, V. Barone, B. Mennucci, G. A. Petersson, H. Nakatsuji, M. Caricato, X. Li, H. P. Hratchian, A. F. Izmaylov, J. Bloino, G. Zheng, J. L. Sonnenberg, M. E. M. Hada, , K. F. R. Toyota, J. Hasegawa, M. Ishida, T. Nakajima, Y. Honda, O. Kitao, H. Nakai, T. Vreven, J. Montgomery, J. E. Peralta, F. Ogliaro, M. Bearpark, J. J. Heyd, E. Brothers, K. N. Kudin, V. N. Staroverov, R. Kobayashi, J. Normand, K. Raghavachari, A. Rendell, J. C. Burant, S. S. Iyengar, J. Tomasi, M. Cossi, N. Rega, N. J. Millam, M. Klene, J. E. Knox, J. B. Cross, V. Bakken, C. Adamo, J. Jaramillo, R. Gomperts, R. E. Stratmann, O. Yazyev, A. J. Austin, R. Cammi, C. Pomelli, J. W. Ochterski, R. L. Martin, K. Morokuma, V. G. Zakrzewski, G. A. Voth, P. Salvador, J. J. Dannenberg, S. Dapprich, A. D. Daniels, Ö. Farkas, J. B. Foresman, J. V. Ortiz, J. Cioslowski and D. J. Fox, *Gaussian 09*, Gaussian.

2 F. Jia, Z. He, L.-P. Yang, Z.-S. Pan, M. Yi, R.-W. Jiang and W. Jiang, *Chem. Sci*., 2015, **6**, 6731.

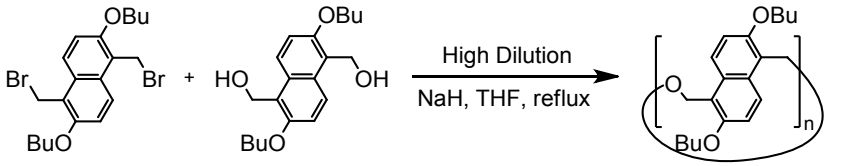

The same synthetic procedure as used for the synthesis of **TA4** was employed here.[1] To the mixture of NaH (0.43 g, 18 mmol) and Cs_2CO_3 (5.9 g, 18 mmol) in dry THF (400 mL) at reflux was added the solution of dibromide **1** (1.4 g, 3.0 mmol) and diol **2** (1.0 g, 3.0 mmol) in dry THF (60 mL) dropwise through a syringe pump during 6 h. The resulting mixture was stirred at reflux for another 60h. The solvent was removed under reduced pressure. The residue was suspended in H_2O (30 mL), and then extracted with CH_2Cl_2 (30mL×3). The combined organic phase was washed with saturated NaCl and dried over anhydrous Na_2SO_4. Then, the solvent was removed with rotary evaporator to give the crude product which was purified several times by column chromatography (SiO_2, petroleum ether: ethylacetate = 8:1 ~ 3:1) to give pure *per*-butyl oxatub[5]arene (**TA5**) and *per*-butyl oxatub[6]arene (**TA6**).

TA5: a white solid (20 mg, 1.1%).^{1}H NMR (400 MHz, CD_2Cl_2, 25 ^{o}C): δ [ppm] = 7.80 (d, J = 9.3 Hz, 10H), 6.97 (d, J = 9.3 Hz, 10H), 4.98 (s, 20H), 3.82 (t, J = 6.4 Hz, 20H), 1.63 – 1.56 (m, 21H), 1.40 – 1.33 (m, 20H), 0.87 (t, J = 7.4 Hz, 30H). ^{13}C NMR (100 MHz, CD_2Cl_2, 25 ^{o}C): δ [ppm] = 153.34, 129.33, 126.09, 119.49, 115.34, 69.44, 61.79, 31.61, 19.25, 13.65. ESI-TOF-HRMS: *m/z* calcd for $[M+K]^+$ $C_{100}H_{130}O_{15}K^+$, 1609.9041; found 1609.9107 (Error = 4.1 ppm). Elemental Analysis: calcd for $C_{100}H_{130}O_{15}$: C 76.40, H 8.33; found C 76.56, H 8.35 (For C, Error = 0.2%).

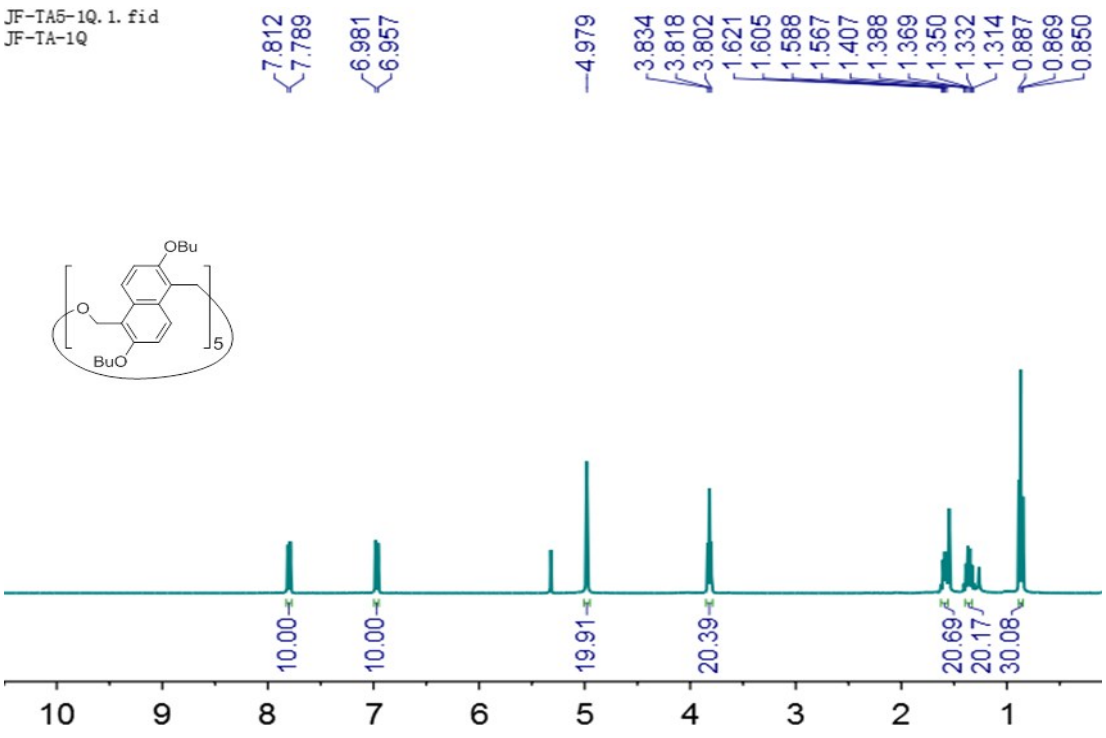

^{1}H NMR spectrum (400 MHz, CD_2Cl_2, 25 °C) of **TA5**.

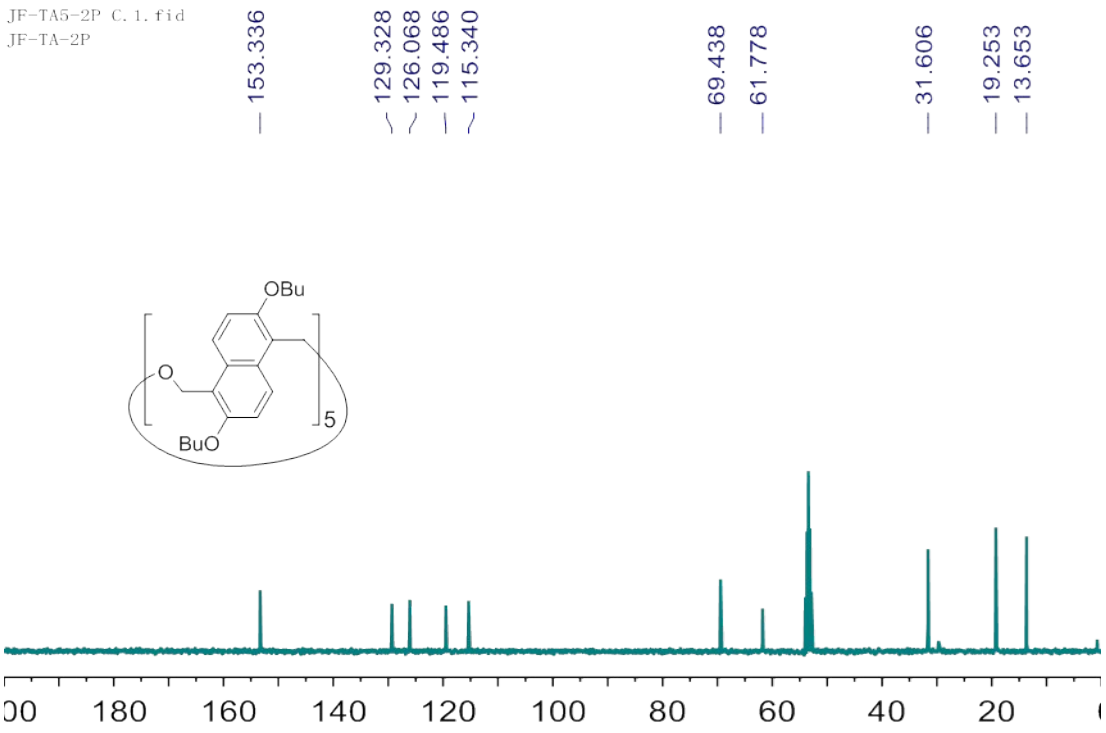

^{13}C NMR spectrum (100 MHz, CD_2Cl_2, 25 °C) of **TA5**.

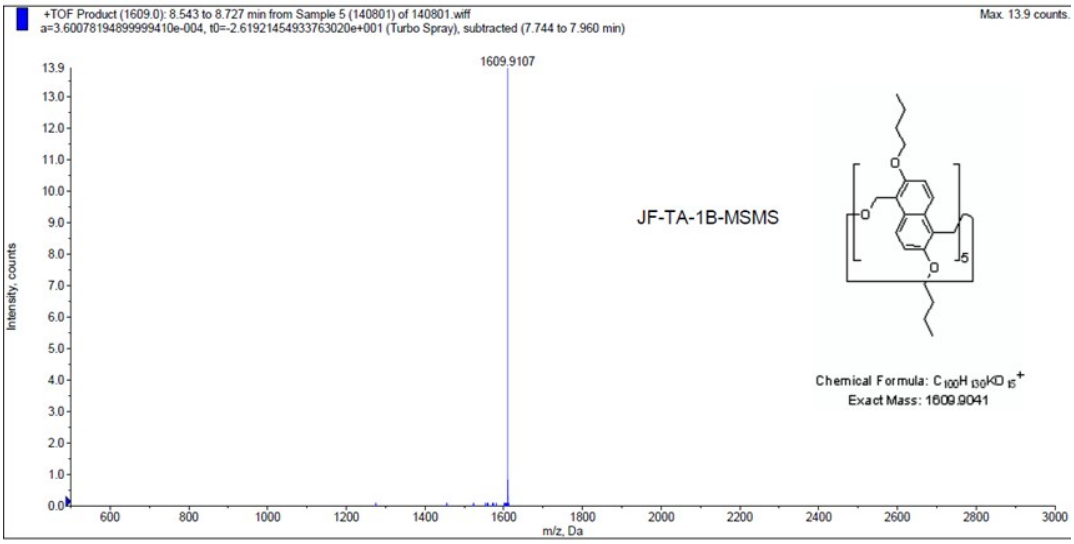

ESI-TOF mass spectrum of **TA5**.

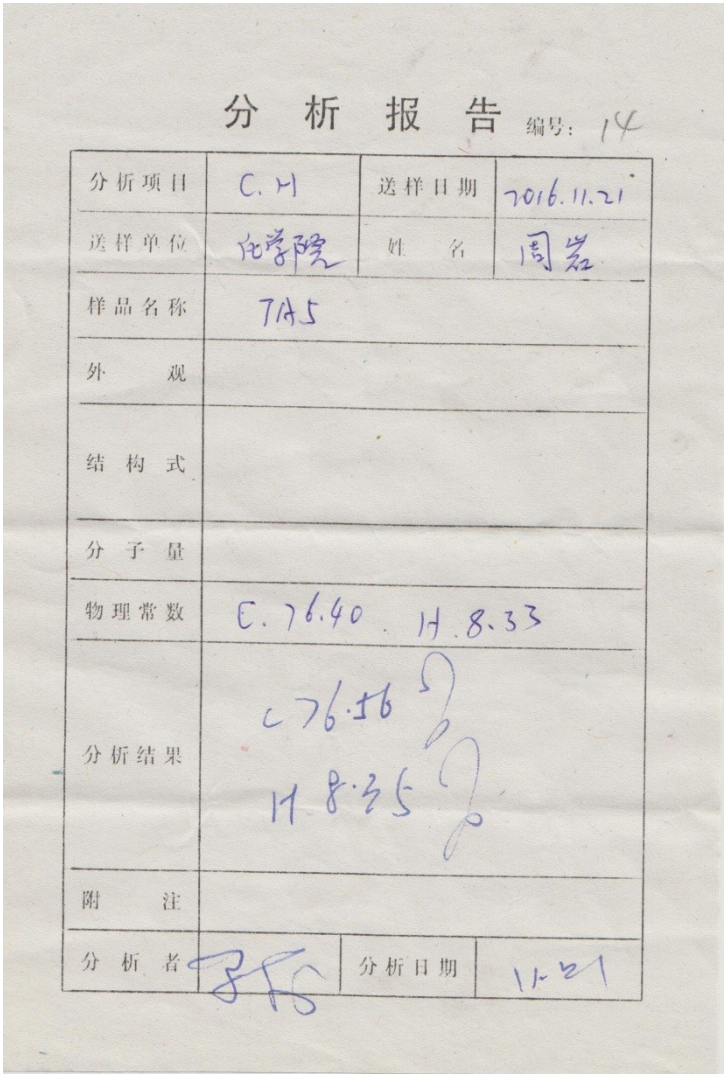

分 析 报 告 编号：14

分析项目	C. H	送样日期	2016.11.21
送样单位	化学院	姓 名	周岩
样品名称	TA5		
外 观			
结 构 式			
分 子 量			
物理常数	C. 76.40 H. 8.33		
分析结果	C 76.56 H 8.25		
附 注			
分 析 者		分析日期	11-21

Elemental analysis of **TA5**.

TA6: a white solid (65 mg, 3.4%). ^{1}H NMR (400 MHz, CD_2Cl_2, 25 ^{o}C): δ [ppm] = 7.80 (d, J = 9.3 Hz, 12H), 6.98 (d, J = 9.3 Hz, 12H), 4.96 (s, 24H), 3.87 (t, J = 6.4 Hz, 24H), 1.66 – 1.59 (m, 24H), 1.43 – 1.36 (m, 24H), 0.88 (t, J = 7.4 Hz, 36H). ^{13}C NMR (100 MHz, CD_2Cl_2, 25 ^{o}C): δ [ppm] = 153.81, 129.74, 126.66, 119.78, 115.79, 69.90, 62.25, 32.03, 19.66, 14.04. ESI-TOF-HRMS: *m/z* calcd for $[M+K]^+$ $C_{120}H_{156}O_{18}K^+$, 1924.0923; found 1924.0889 (Error = -1.8 ppm). Elemental Analysis: calcd for $C_{120}H_{156}O_{18}$: C 76.40, H 8.33; found C 76.47, H 8.41 (For C, Error = 0.09%).

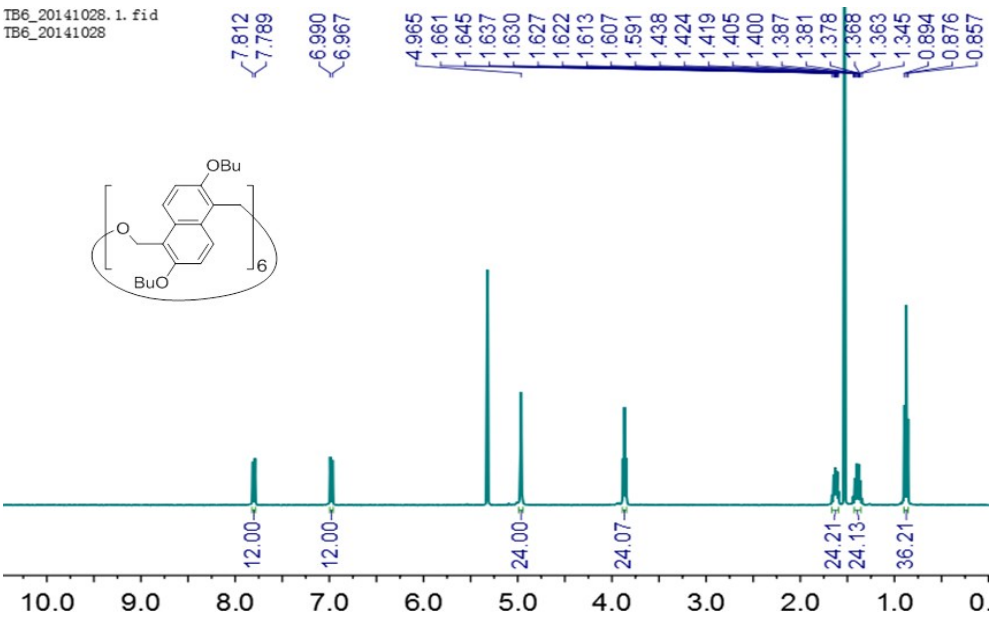

^{1}H NMR spectrum (400 MHz, CD_2Cl_2, 25 ^{o}C) of **TA6**.

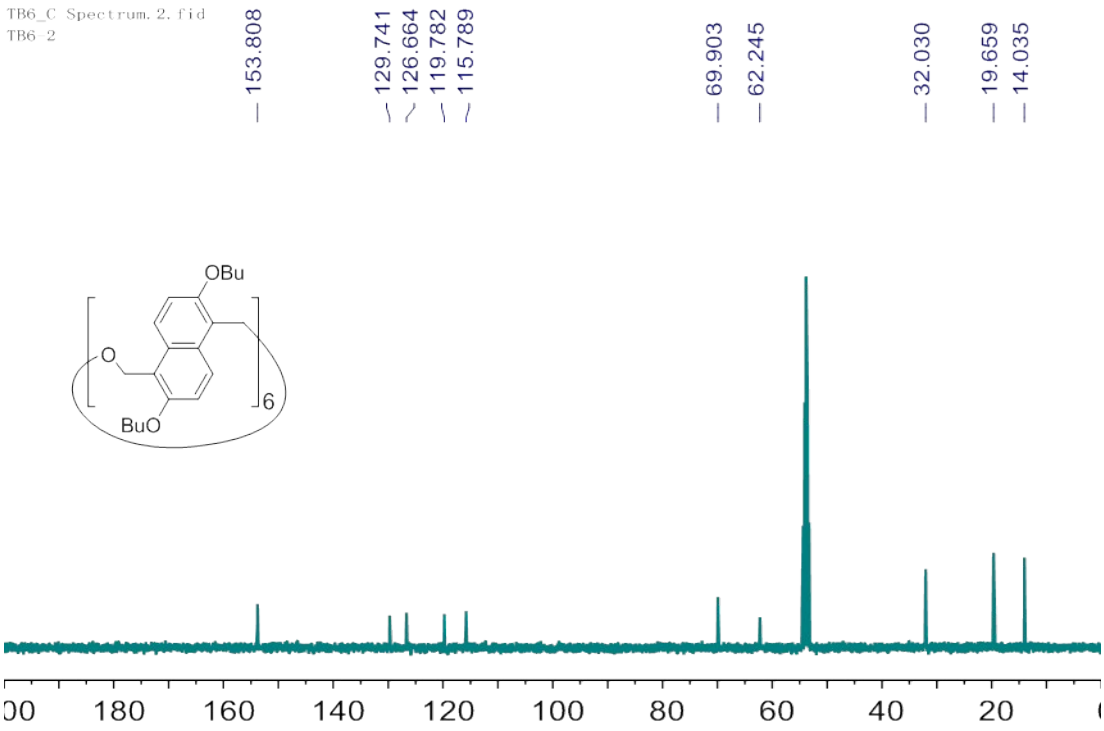

^{13}C NMR spectrum (100 MHz, CD_2Cl_2, 25 ^{o}C) of **TA6**.

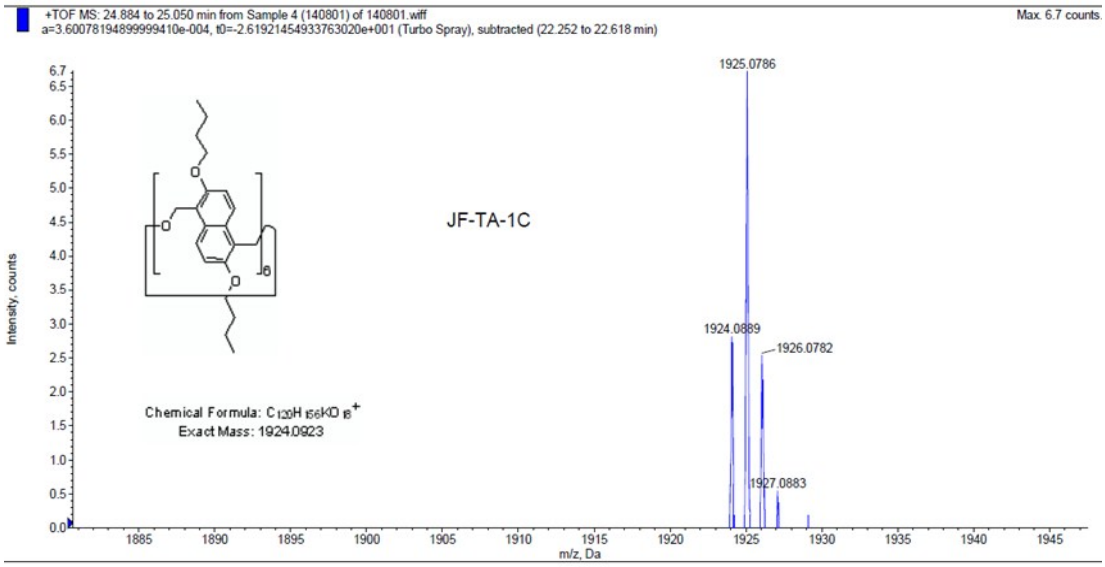

ESI-TOF mass spectrum of **TA6**.

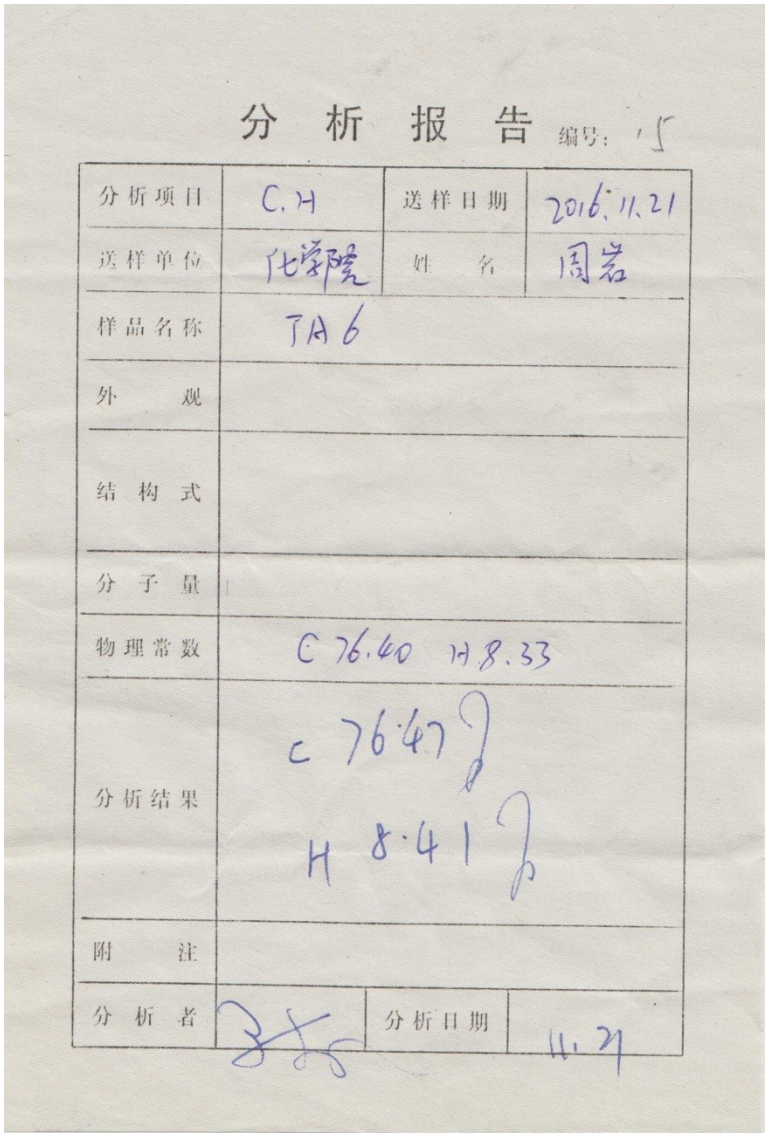

分析报告 编号：15

分析项目	C, H	送样日期	2016.11.21
送样单位	化学院	姓名	周岩
样品名称	TA6		
外观			
结构式			
分子量			
物理常数	C 76.60 H 8.33		
分析结果	C 76.47 H 8.41		
附注			
分析者		分析日期	11.21

Elemental analysis of **TA6**.

2. ^{1}H NMR of the Diol 2 Containing Impurity

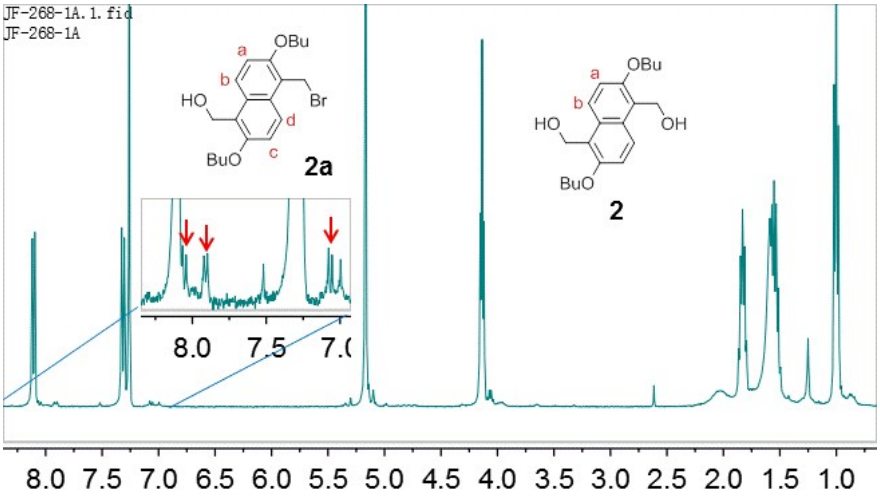

Figure S1 ^{1}H NMR spectrum (400 MHz, CD_2Cl_2, 25 °C) of the diol **2**. The inset spectrum shows that there is some impurity in the diol. The diol was synthesized through the hydrolysis of the dibromide **1**.[2] Presumably, the impurity is the partially hydrolyzed product **2a** which should have four doublets in the aromatic region: Three of them were observed, and the fourth one may be overlapped with the NMR peaks of the diol **2**.

3. Comparison of TA4, TA5 and TA6

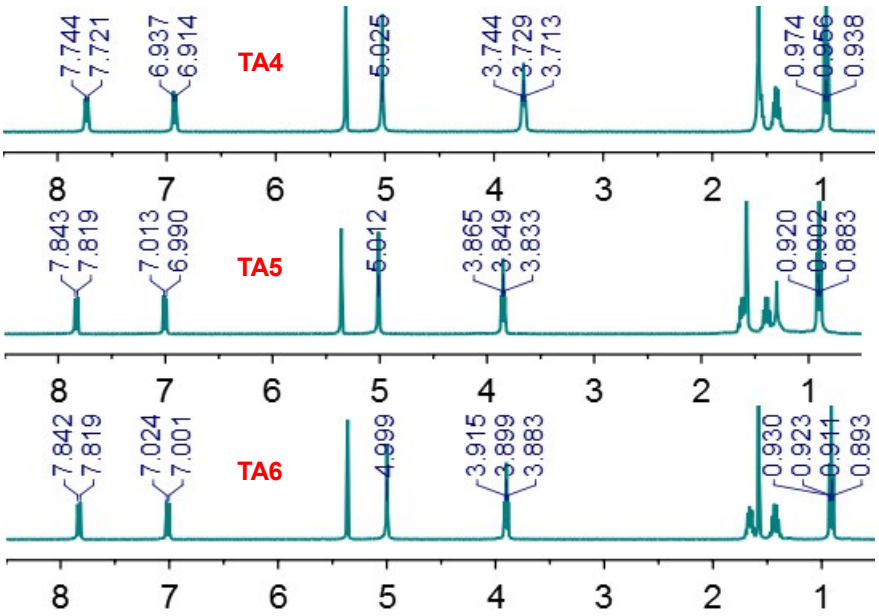

Figure S2 ^{1}H NMR spectra (400 MHz, CD_2Cl_2, 25 °C) of **TA4**, **TA5** and **TA6**. As shown in the figure, compared with **TA4**, the protons (*1*, *2* and *c*) of **TA5** and **TA6** shift a little downfield, while the proton (*a*+*b*) of **TA5** and **TA6** shifts a little upfield.

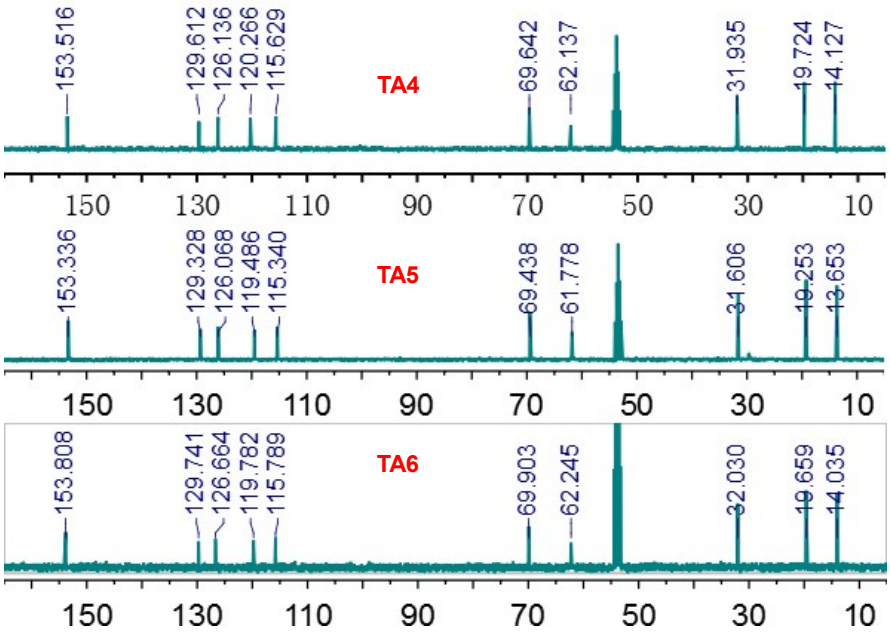

Figure S3 ^{13}C NMR spectra (400 MHz, CD_2Cl_2, 25 °C) of **TA4**, **TA5** and **TA6**. There are also slight differences in their ^{13}C NMR spectra, indicating the cavity sizes and structures are different.

4. Variable Temperature NMR Spectra

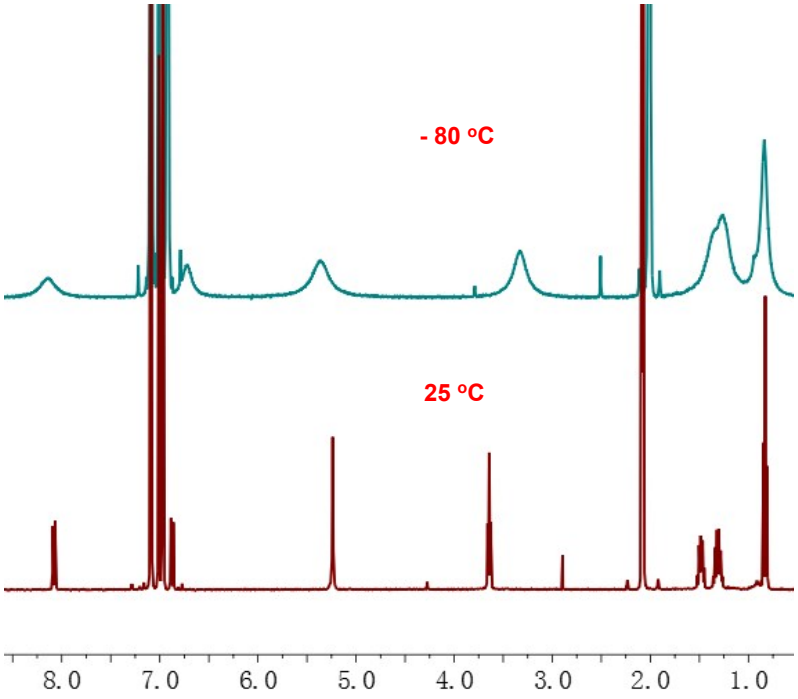

Figure S4 ^{1}H NMR spectra (500 MHz, toluene-d_8) of **TA6** at -80 °C and 25 °C.

5. ^{1}H NMR Spectra of Host-Guest Complexes

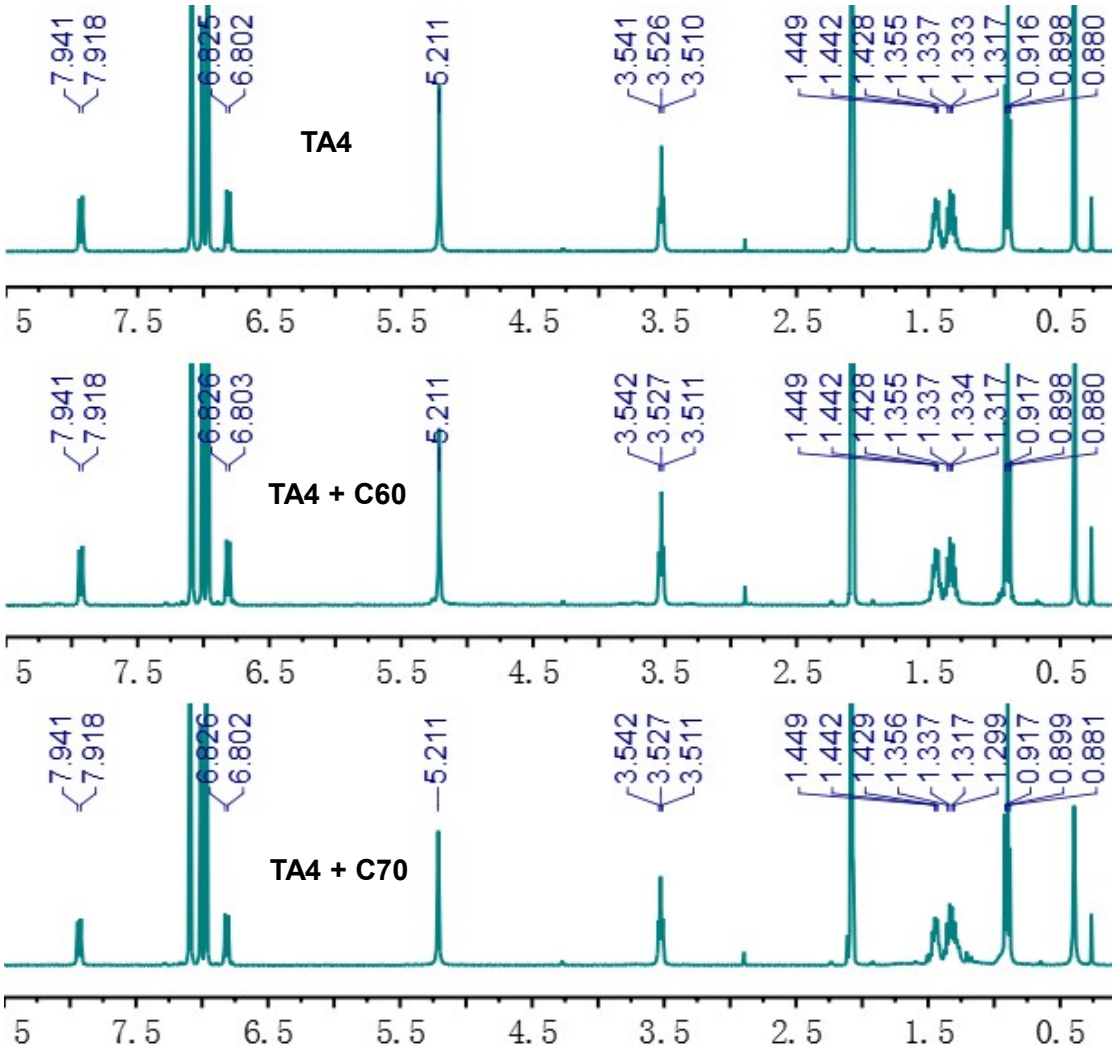

Figure S5 ^{1}H NMR spectra (400 MHz, toluene-d_8, [**TA4**]=1.0 mM, 25 °C) of **TA4**, and 1:2 mixture of **TA4** with **C60** or **C70**. No obvious complexation-induced shifts of the protons on **TA4** were observed, suggesting no complexation between **TA4** and fullerenes (**C60** and **C70**).

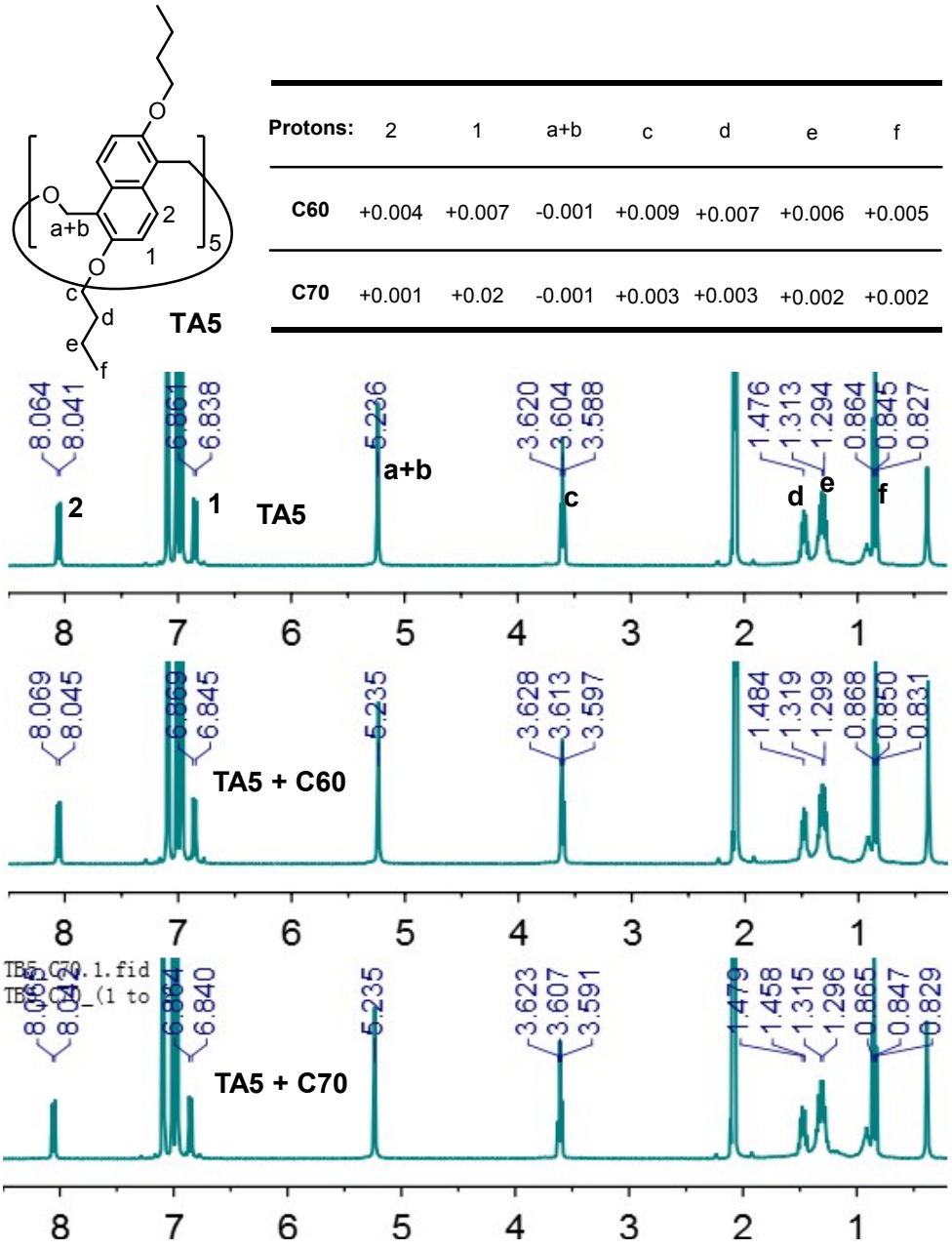

Figure S6 ^{1}H NMR spectra (400 MHz, toluene-d_8, [**TA5**]=1.0 mM, 25 ^{o}C) of **TA5**, and 1:2 mixture of **TA5** with **C60** or **C70**. The complexation-induced shifts of the protons on **TA5** by adding **C60** or **C70** are shown in Table for comparison. Obviously, the complexation-induced shifts are too small to accurately determine the binding constants.

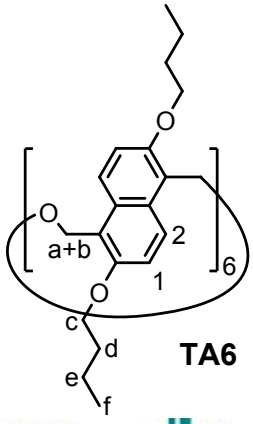

Protons:	2	1	a+b	c	d	e	f
C60	+0.039	+0.081	-0.017	+0.079	+0.066	+0.053	+0.040
C70	+0.041	+0.155	-0.059	+0.171	+0.151	+0.126	+0.101

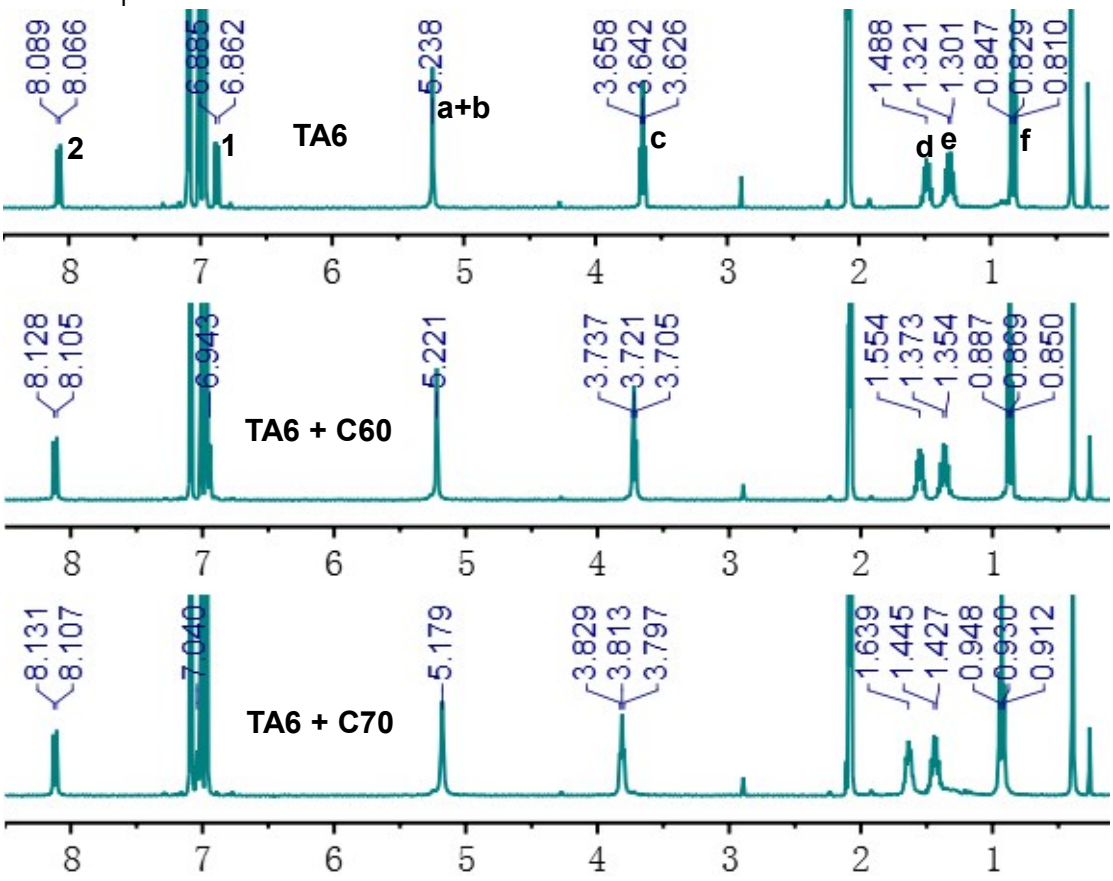

Figure S7 ^{1}H NMR spectra (400 MHz, toluene-d_8, [**TA6**]=1.0 mM, 25 ^{o}C) of **TA6**, and 1:2 mixture of **TA6** with **C60** or **C70**. The complexation-induced shifts of the protons on **TA6** by adding **C60** or **C70** are shown in Table for comparison. Obviously, the large shifts suggest that **TA6** can complex with **C60** or **C70**.

6. Determination of Binding Constants

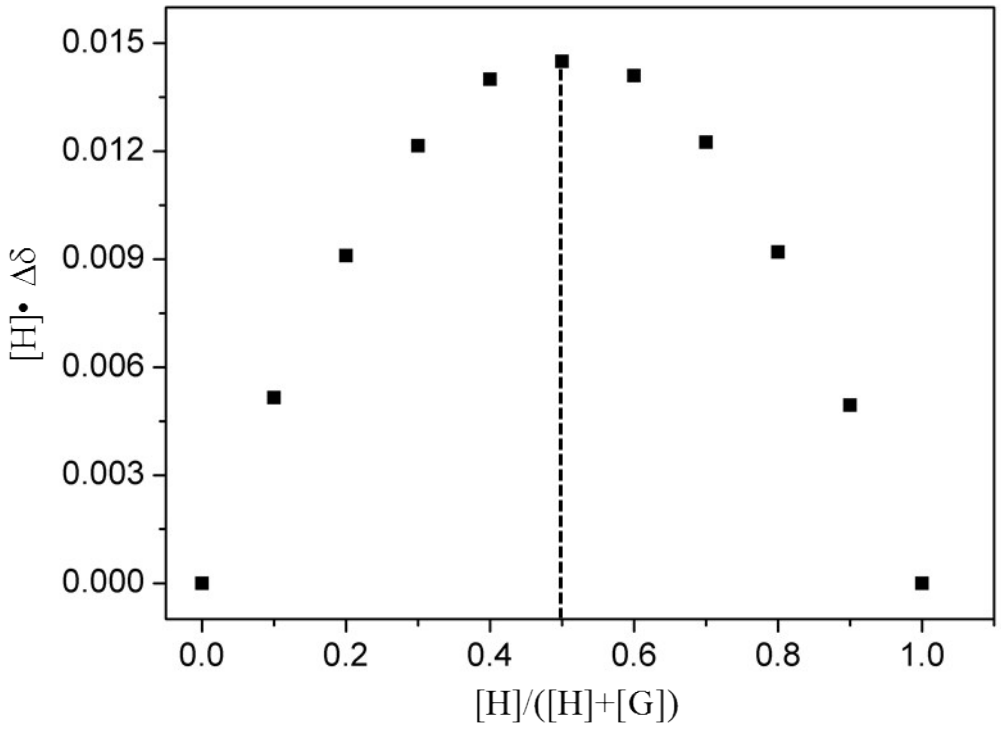

Figure S8 Job's plot obtained by plotting the chemical shift change ($\Delta\delta$) of the Host's proton *c* in ^{1}H NMR spectra by varying the ratio of the host and the guest against the mole fraction of **TA6**. The total concentration of the host and the guest is fixed: [Host] + [Guest] = 1.0 mM. This experiment supports the 1:1 binding stoichiometry between **C70** and **TA6** in the Toluene-d_8.

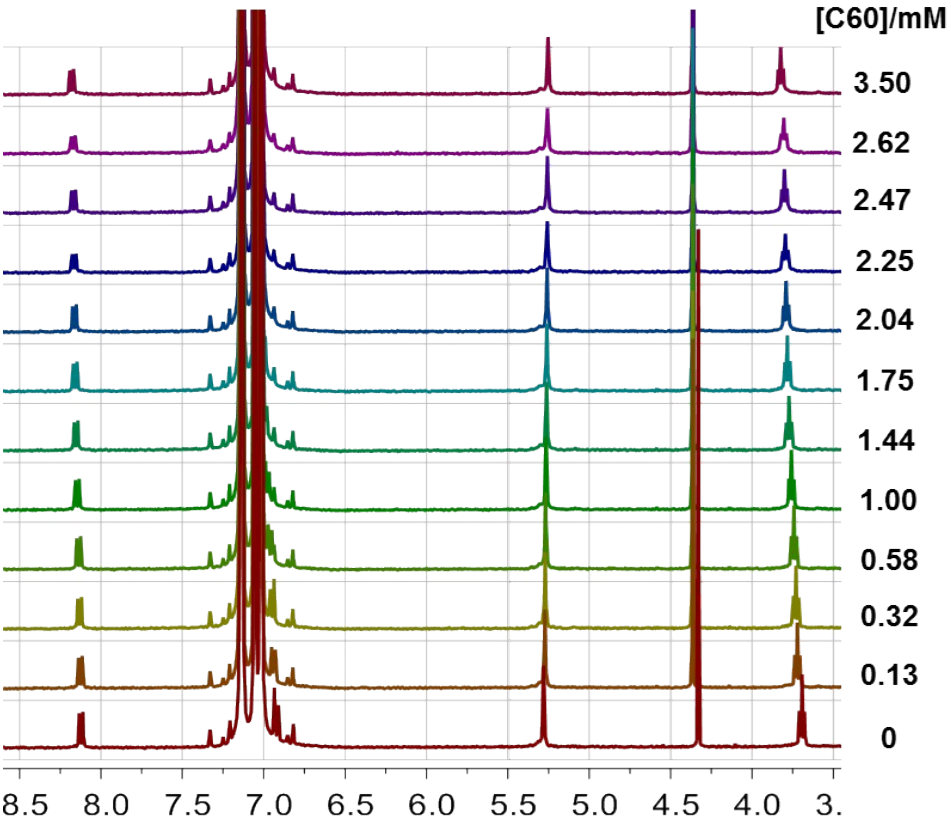

Figure S9 Partial ^{1}H NMR spectra (400 MHz, Toluene-d_8, 25 ^{o}C) of **TA6** (0.10 mM) titrated by **C60**. From bottom to top, the concentration of **C60** was 0~3.5 mM. Proton *2* of **TA6** was monitored during the titration for the calculation of binding constants, which is the same for all the following experiments, unless otherwise noted. Nonlinear curve-fitting method used here has been reported.[3] Note: Since the solubilities of **C60** (2.8mg/mL, 25 ^{o}C) and **C70** are poor in toluene,[4] it is not possible to make their solution in very high concentrations. Addition of the solution of **C60** or **C70** in large volume will perturb the concentration of **TA6**. In order to avoid this, **TA6** was also added to the stock solution of guests and is kept at the same concentration as the titrated **TA6** solution. In this way, when large volume of guest solution was titrated into the solution of **TA6**, the concentration of **TA6** is kept constant.

---

3 G. Huang, Z. He, C.-X. Cai, F. Pan, D. Yang, K. Rissanen and W. Jiang, *Chem. Commun*., 2015, **51**, 15490.

4 R. S. Ruoff, D. S. Tse, R. Malhotra, and D. Lorents, *J. Phys. Chem.*, 1993, **97**, 3379.

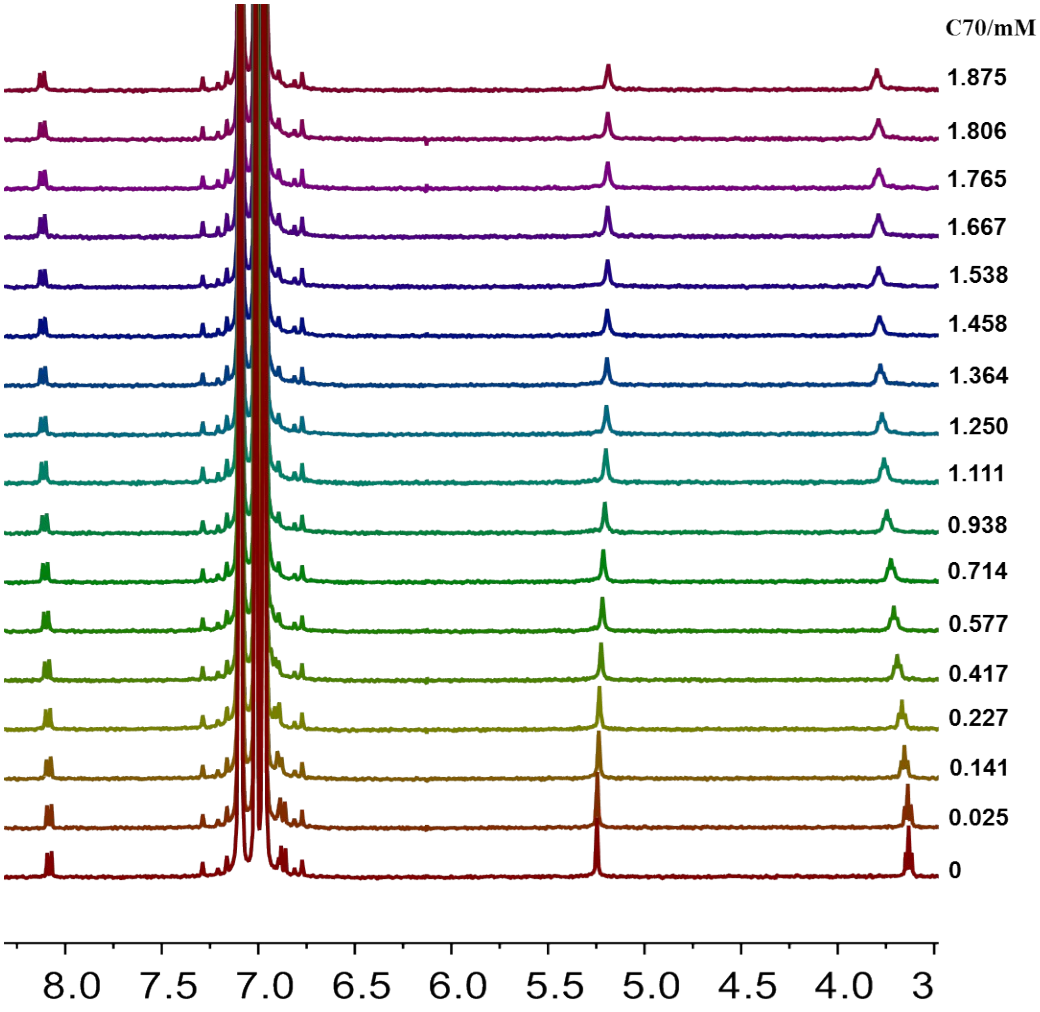

Figure S10 Partial ^{1}H NMR spectra (400 MHz, Toluene-d_8, 25 ^{o}C) of **TA6** (0.1 mM) titrated by **C70**. From bottom to top, the concentration of **C70** was 0~1.875 mM.

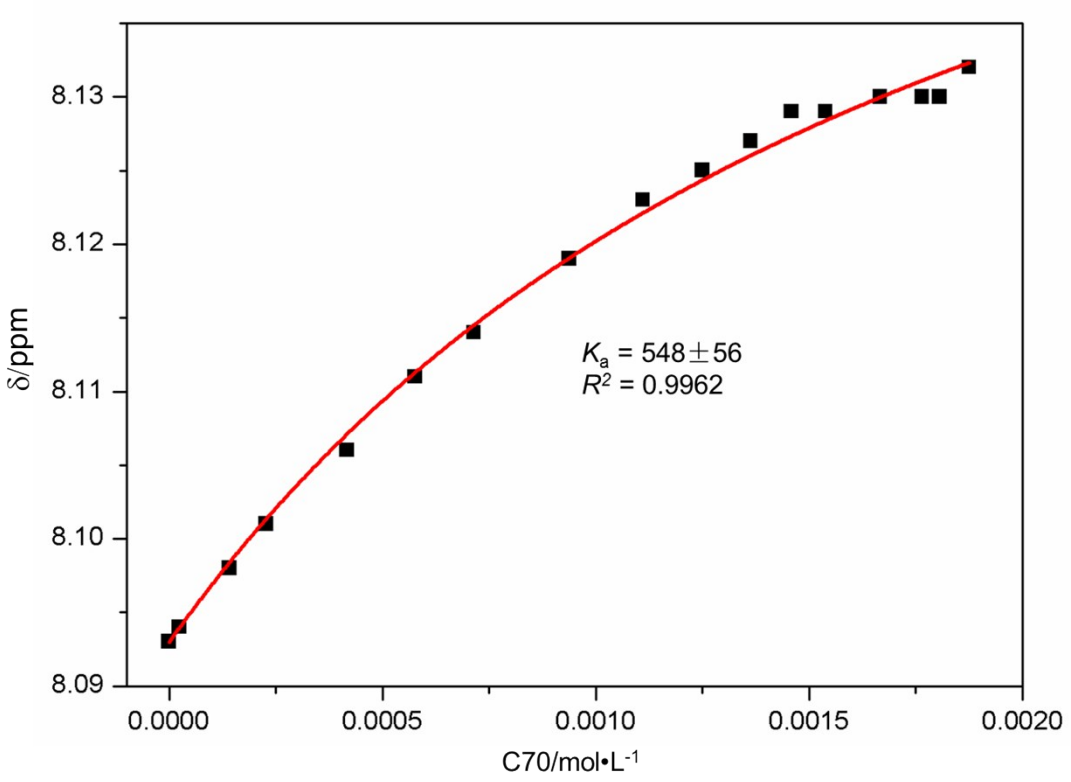

Figure S11 Non-linear curve-fitting for the complexation between **C70** and **TA6** in Toluene-d_8 at 25 °C.

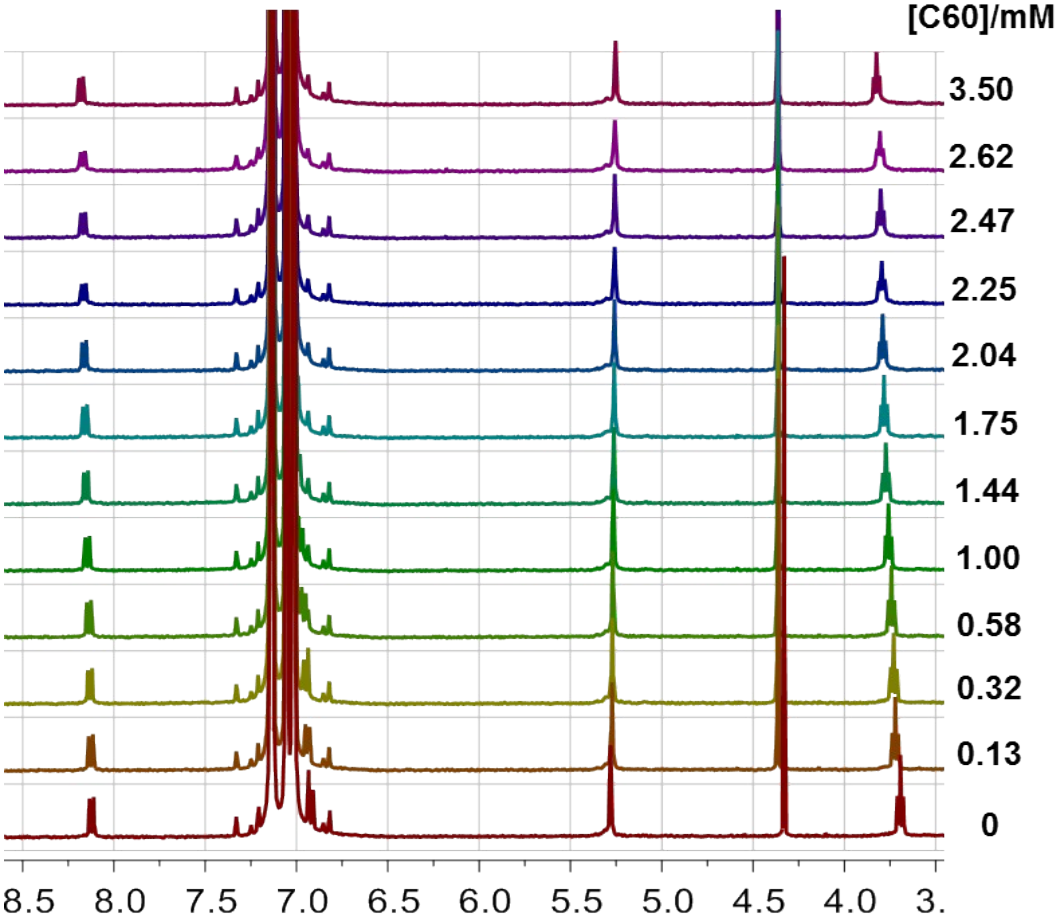

Figure S12 Partial ^{1}H NMR spectra (400 MHz, Toluene-d_8, 35 ^{o}C) of **TA6** (0.1 mM) titrated by **C60**. From bottom to top, the concentration of **C60** was 0~3.5 mM.

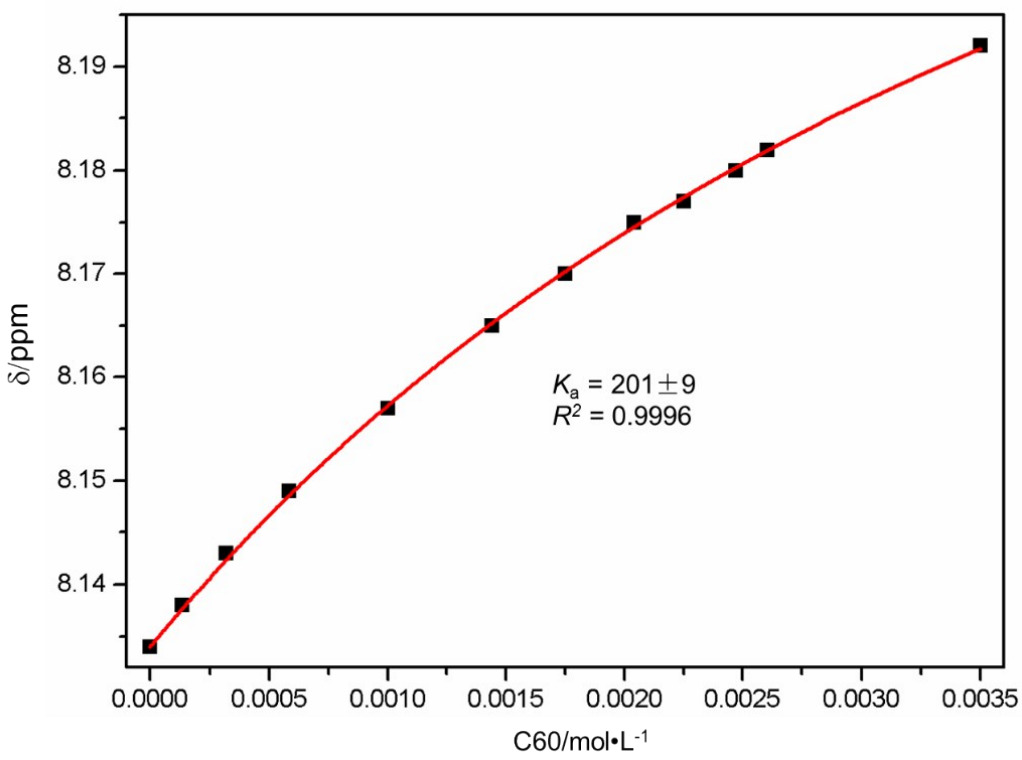

Figure S13 Non-linear curve-fitting for the complexation between **C60** and **TA6** in Toluene-d_8 at 35 °C.

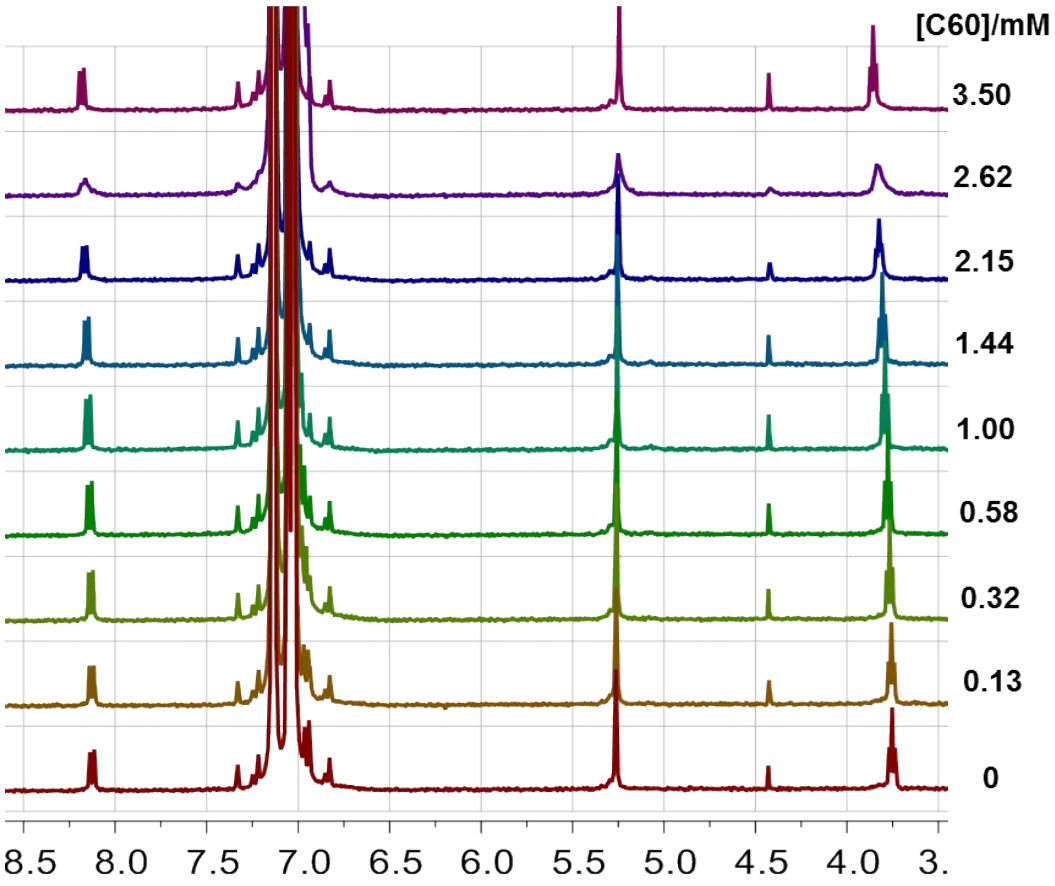

Figure S14 Partial ^{1}H NMR spectra (400 MHz, Toluene-d_8, 45 ^{o}C) of **TA6** (0.1 mM) titrated by **C60**. From bottom to top, the concentration of **C60** was 0~3.5 mM.

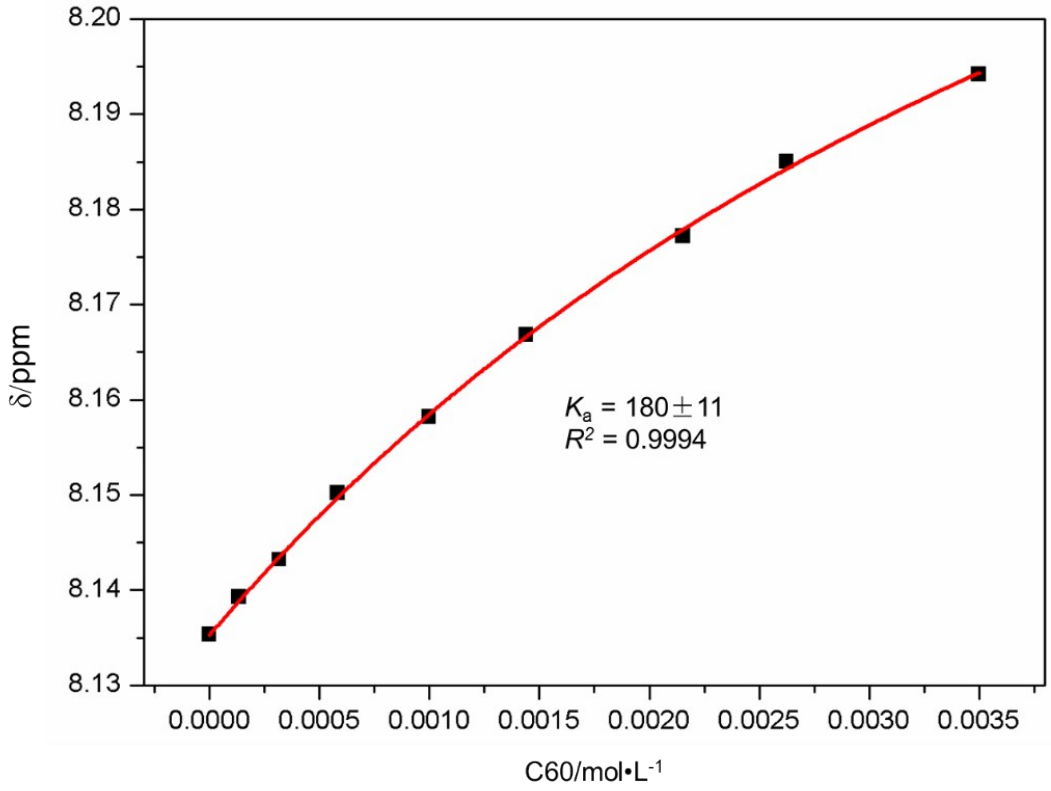

Figure S15 Non-linear curve-fitting for the complexation between **C60** and **TA6** in Toluene-d_8 at 45 °C.

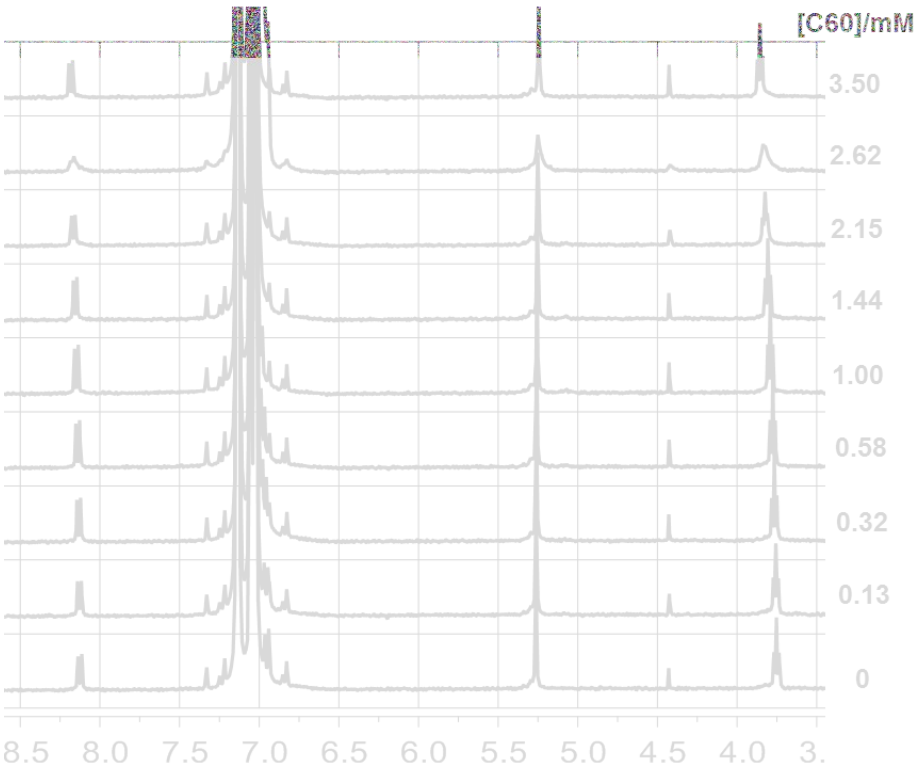

Figure S16 Partial ^{1}H NMR spectra (400 MHz, Toluene-d_8,55 ^{o}C) of **TA6** (0.1 mM) titrated by **C60**. From bottom to top, the concentration of **C70** was 0~3.5 mM.

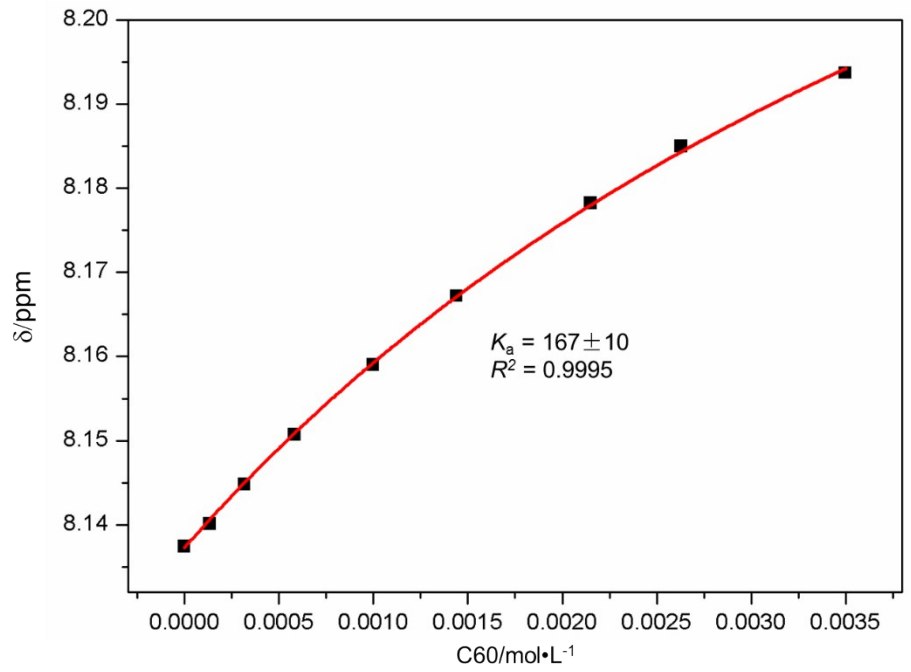

Figure S17 Non-linear curve-fitting for the complexation between **C60** and **TA6** in Toluene-d_8 at 55 °C.

7. Computational Results

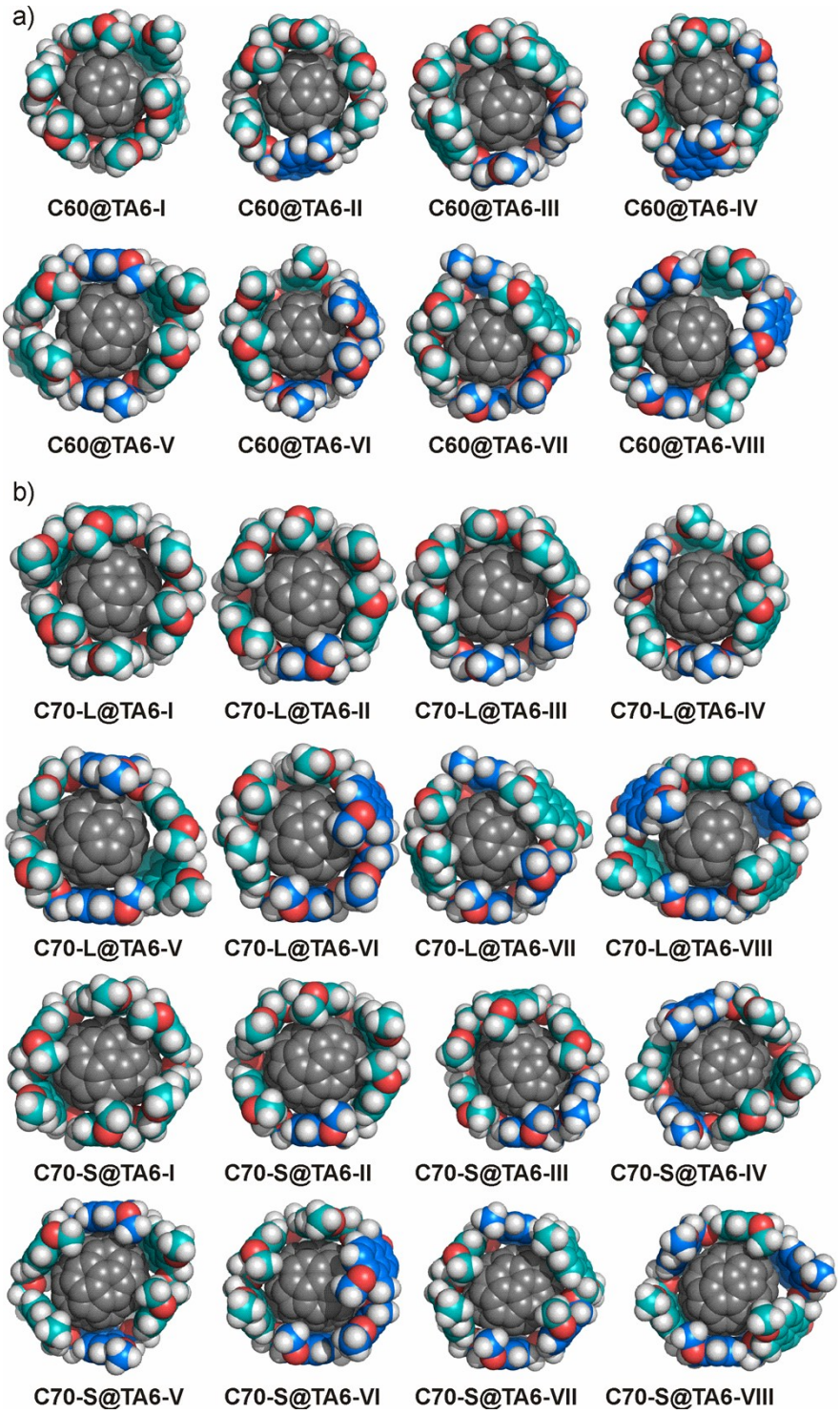

Figure S18. Optimized geometries of the complexes of (a) **C60** or (b) **C70** at the cavity of each conformer of **TA6** (along the long axis: **C70-L@TA6**; along the short one: **C70-S@TA6**) at the BMK/6-31G level of theory by Gaussion 09.